Cost analysis and manufacturing process of blade prototypes with different structural configurations for a 1 kW H-type vertical axis wind turbine

Giovanni Vidal-Flores *, Farid Quijada-Escamilla, Jose Rafael Gomez-Bautista, Isaías Alvarado-Medrano

Gerencia de Energía, Centro de Tecnología Avanzada (CIATEQ), El Marqués, Querétaro, México
* Corresponding author: giovanni.vidal@ciateq.mx

Received: November 1, 2024 Accepted: October 6, 2025 Published: November 27, 2025
DOI: https://doi.org/10.56845/rebs.v7i2.643

Abstract: This article analyzes the costs associated with the manufacturing processes of prototype blades, each measuring 2 meters in length and featuring a NACA 0015 aerodynamic profile, with different structural configurations for a 1 kW H-type vertical axis wind turbine (VAWT). The research identifies the material costs and mass of the blades in order to optimize their manufacturing and achieve efficient performance. The objective is to improve resource efficiency in both research and industrial processes. Two manufacturing methods are evaluated: hand lay-up molding (Prototype A) and vacuum-assisted resin transfer molding (VARTM, Prototypes B and C). The evaluation criteria included manufacturing cost, weight, and quality. Prototype A, a single-piece blade with an EPS core, showed the lowest mass (5.11 kg) and cost, though it required significant surface repairs due to resin slippage, which could affect aerodynamic performance. Prototypes B and C, produced by VARTM with a double-shell design, achieved superior surface quality and a controlled fiber-to-resin ratio (100:50). Prototype B weighed 5.81 kg, while Prototype C, reinforced with a polyurethane core for greater rigidity, was the heaviest at 7.22 kg. However, their manufacturing costs were considerably higher: 215% (B) and 312% (C) compared to Prototype A, mainly due to the use of specialized materials. The results highlight the trade-offs between cost, mass, and quality, offering a reference for the development of structurally efficient and economically viable VAWT blades for urban applications. The conclusions are especially relevant for guiding future design and manufacturing decisions for VAWTs intended to operate in challenging environments characterized by turbulent and low-speed winds.

Keywords: VAWT, composite materials enhancement, VARTM procedure, blade manufacture, cost analysis.

Introduction

Wind energy is one of the most important sources of renewable energy worldwide. The two primary configurations of wind turbines used to harness wind energy are Vertical Axis Wind Turbines (VAWTs) and Horizontal Axis Wind Turbines (HAWTs). Each configuration has its own advantages and disadvantages. The main advantages of VAWTs over HAWTs include their omnidirectionality—allowing them to capture wind from any direction—as well as their suitability for lower wind speeds and urban environments. In addition, VAWTs offer a more compact design, generate lower noise levels, and are generally easier to maintain. On the other hand, the design of VAWTs can result in higher structural stress and significant torque fluctuations, which may affect their reliability and lifespan. Nevertheless, continued investment in VAWT technology has the potential to drive innovations that enhance efficiency, durability, and cost-effectiveness while reducing environmental impact. Such advancements could open new markets and complement existing wind technologies, ultimately contributing to a more diverse and resilient renewable energy landscape.

Since the development of the Savonius and Darrieus types of VAWTs in the 1930s, several alternative designs have emerged in pursuit of higher efficiency, including the H-rotor and the helicoidal rotor. The first wave of experimental research, prototype testing, and commercial models took place during the 1980s and 1990s, with the introduction of the Φ-type VAWT rotor. By 2010, commercial H-type VAWT rotors were deployed for small-scale electricity generation (Stoevesandt *et al.*, 2020). In recent years, renewed interest in VAWTs has emerged, with two major applications being identified: advancements in offshore installations and the development of small-scale VAWTs designed for highly turbulent environments, such as urban areas.

The new interest in VAWT technology is towards offshore applications due to the great wind potential at sea, allowing the development of this type of technology on a large scale and taking as a reference the offshore wind energy installation prospects in Europe for 2023-2027 with a capacity of 129 GW (Brandetti, 2024). Some research has been conducted on the challenges due to the harsh environment, as well as on the analysis of experimental prototypes (Ghigo *et al.*, 2024), studies on the design of floating offshore wind turbine platforms (Edwards *et al.*, 2024), innovative design of a lightweight modular floating foundation for offshore VAWTs to reduce operating costs (Boo *et al.*, 2023),

and on the development of numerical design and analysis tools to ensure engineering for aero-hydro-servo-elastic simulations of VAWT (Devin, 2023).

With the new challenges to mitigate energy deficiency in areas with little infrastructure and even for the development of "smart cities" or the implementation of smart grids, the development of smart wind farms with VAWT has been chosen, specifically in areas where there is a low wind speed or high turbulence. Nowadays, several commercial models of VAWT are marketed, manufacturing components (such as blades) with some conventional materials such as aluminum and composite materials, both with advantages and disadvantages according to the operation conditions.

VAWT applications in turbulent environments such as urban and rural areas have great potential on a large-scale to supply power to buildings, street lighting or to store energy for use in other small applications. Additionally, some research has been developed to improve current technology. These research include the development of a design methodology to understand the effect of geometrical parameters in the performance of VAWT (Cuevas-Carvajal *et al.*, 2022), improving the aerodynamic efficiency of VAWT with numerical simulations of new blade designs without an expensive manufacturing process (Mendoza and Bernhoff, 2020), a proposals of roof top building modifications based on CFD analysis for the installation of VAWTs to increase wind energy harvesting in urban areas (Juan *et al.*, 2024), structural optimization of H-type VAWT rotor to reduce blade mass and avoid peak stresses and strain limits (Marzec *et al.*, 2023) and optimizing efficiency using fixed deflector fins by reducing production materials and maximizing annual energy production (AEP) (Marinić-Kragić *et al.*, 2022), including algorithms that define an optimal structural design of the blade with the parameters of laminate thickness, reinforcement orientation, Fiber-to-Volume Fraction (FvF), resin matrix and number of reinforcement layers (Geneid *et al,*. 2022).

Efforts have been made to optimize aerodynamic performance, develop new prototypes, optimize costs, develop simulation tools, and develop new design and manufacturing methodologies to achieve new applications with VAWT technologies. In this work, an analysis is shown to find a balance between material costs and low mass criteria for a VAWT that could take advantage of low speeds with good long-term performance. The aim is to save resources in manufacturing processes at the research and industrial level.

Furthermore, this report serves as a model for those developers such as research centers, academia, small industry, and independent developers who in their work carry out manufacturing processes of small wind turbines, in such a way that they can take it as a reference to delve into the cost. The long-term goal is to replicate a final design for urban applications with high turbulence environments and low wind speeds, ensuring a good structural design of VAWT blades with a service life in accordance with the IEC 61400-2: Small wind turbines (IEC, 2013).

Materials and Methods

I. Background

Composite materials

Composite materials are formed by combining two or more constituent elements, primarily a matrix and a reinforcement, to enhance their mechanical properties. The most common hand-made composite materials are Polymer Matrix Composites (PMCs), Metal Matrix Composites (MMCs), and Ceramic Matrix Composites (CMCs). These materials can be tailored to achieve specific mechanical properties by carefully selecting their constituents, proportions, distribution, structural arrangement, interfacial composition, and other factors (Chawla, 2019).

The reinforcement is typically in fiber form, being the most common glass fiber; Its primary function is to support loads along the longitudinal direction while providing minimal strength in the transverse direction. Structural reinforcements are **E – glass (electrical)**, **C – glass (chemical)** and **R, S or T – glass (ballistic applications)** (Gurit, 2016). Other forms include carbon, aramid, ceramics, boron, polyester or natural fibers (Chawla, 2019).

The matrix in composite materials can take various forms, including epoxy, polyester, and vinylester. These matrices, commonly referred to as polymers, consist of long chain-like molecules made up of repeated units, often called synthetic resins or simply resins. Resins are generally classified into two types: **thermoplastics**, which undergo a

reversible process (e.g., nylon, ABS, polypropylene), and **thermosets**, which undergo a non-reversible process (e.g., epoxy, polyester) (Gurit, 2016).

Applied loads and stresses are primarily transmitted along the reinforcements, while the matrix protects the reinforcements from environmental degradation and maintains their position within the composite structure (see Figure 1) (Alvarado, 2023).

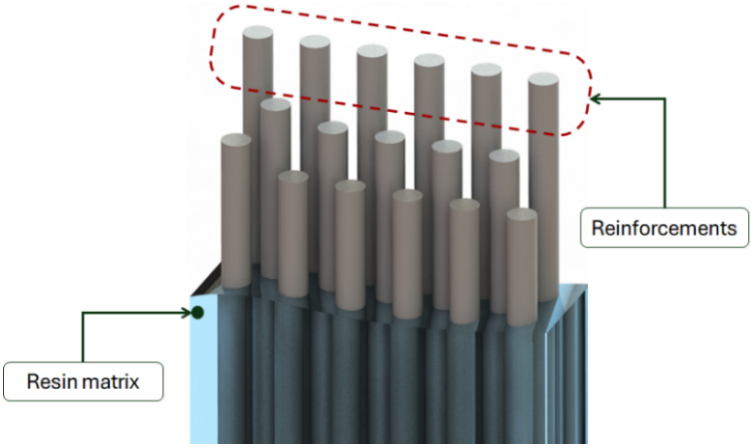

Figure 1. Schematic representation of the general composition of a composite material (matrix and reinforcements).

The Fiber Volume Fraction (FvF) is defined as the ratio of the total volume of reinforcements to the overall volume of the composite material. This parameter is important because it influences the strength and stiffness of the composite and depends on the reinforcement structure (e.g., type of weave) as well as the manufacturing process.

Glass fiber reinforcements in wind industry

For wind energy industry applications, the most widely used are continuous fibers. These reinforcements have a commercial presentation in the form of a ply, where these reinforcements are woven to create a ply with a specific orientation according to application requirements. Typical orientations are shown in Figure 2:

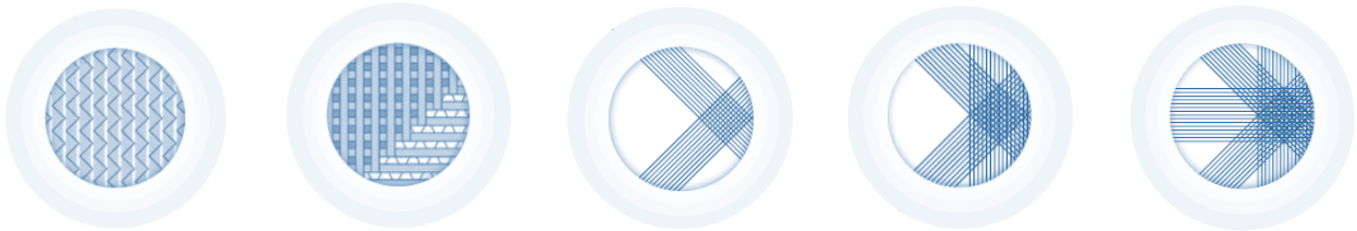

Figure 2. Typical orientation of continuous fiber reinforcements (Gurit, 2016).

Resin Matrix in wind industry

Thermoset epoxy resins are widely used in the wind industry, in the manufacturing and repairing processes for wind turbine blades, thanks to their excellent manufacturing flexibility and mechanical properties (KUKDO, 2011).

II. Process definition

Several production processes exist in wind industry to obtain the final product. These processes can be classified into open molding and closed molding as shown in the Table 1:

Table 1. Manufacturing methods with composite materials (Lee *et al.*, 2021).

Open molding	Closed molding
• Hand lay-up • Filament winding • Spray up	• Pre-preg • Resin transfer molding (RTM) • Vacuum infusion • Compression molding • Pultrusion

The Wind Energy Innovation Laboratory at CIATEQ has the infrastructure to carry out two types of manufacturing processes with composite materials: the hand lay-up and the Vacuum Assisted Resin Transfer Molding (VARTM). The VARTM process is widely employed in the production of wind turbine blades, ranging from small to large scales.

Hand lay-up process

In this process, the resin is manually poured over the fiberglass layers and then distributed across the entire surface using impregnation rollers. This process is among the most cost-effective in the industry, as it requires relatively few consumables, tools or specialized equipment, and the primary materials are inexpensive. However, achieving proper lamination requires skill to ensure uniform fiber impregnation and to avoid excessive application of the resin matrix.

VARTM process

This process requires a mold with the shape of the component and consumables as depicted in Figure 3. The general steps of this process are as follows:

Step 1: Prepare the mold surface (1) before applying the fiberglass layers with release film, then place the tacky-tape (2) over the perimeter on the mold surface.
Step 2: Stack the fiberglass layers (3) according to the laminate drawings.
Step 3: Place the consumables on the laminate according to the infusion diagrams; peel-ply (4), runner (5), inlet and outlet hose (6,7).
Step 4: Tape the vacuum-bag (8) with the tacky-tape (2), make sure there are no gaps that allow air to enter.
Step 5: Connect the outlet hose (7) with the vacuum pump (9,10) to extract the air from inside the vacuum-bag (8) by compacting the stacked fiberglass layers (3).
Step 6: Perform a vacuum test before allowing the entry of epoxy resin.
Step 7: Mix the epoxy resin (11) and connect directly to the inlet hose.
Step 8: Control the process infusion (12) until all the fiberglass layers are completely impregnated.
Step 9: Control the temperature for the curing process
Step 10: Demolding, trimming, dimensional control and painting process.

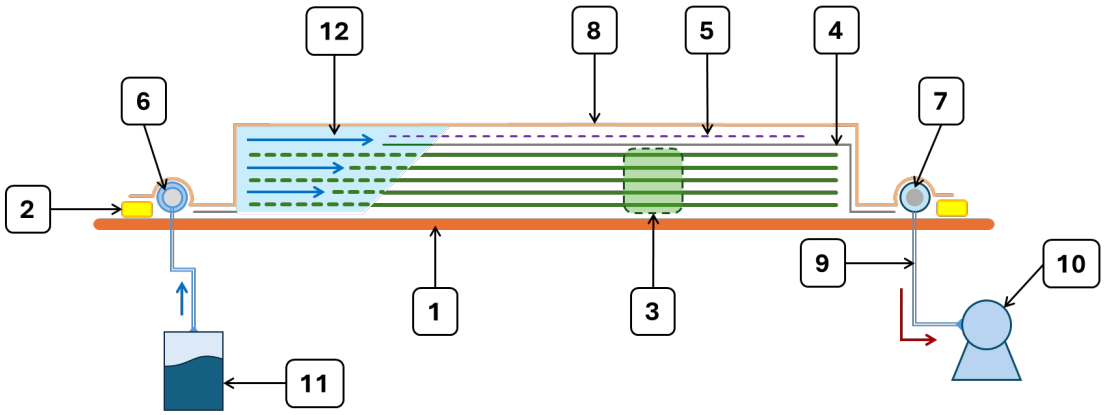

Figure 3. Elements of a VARTM process.

III. Experimental Set-up

The experimental configuration for this work was designed to compare the costs associated with two manufacturing methods for the fabrication of a blade model (see Table 2 for characteristics of the VAWT blade): Hand lay-up process (Prototype A) and VARTM process. The VARTM method was further evaluated in two variants: Prototype B (without shear web) and Prototype C (with shear web). The evaluation criteria considered included manufacturing cost, weight and quality associated to each process. According to a previous study, weight is an important factor in achieving a low starting torque at low wind speeds for the design of a 1 kW VAWT (Vidal-Flores y Hernández-Arriaga, 2024).

Prototypes A, B, and C utilize continuous E-glass fiber reinforcements oriented in unidirectional (0°) and biangular (+45°/-45°) configurations. The reinforcement fibers were supplied by SAERTEX, a commercial brand providing materials for wind energy applications in Mexico. The resin matrix was supplied by KUKDO CHEMICAL HQ. The details of the manufacturing process are described in the following sections.

Table 2. General characteristics of the VAWT blade.

Characteristic	Data
Blade span	2 m
Airfoil	NACA 0015
Chord	20 cm
Materials	Fiberglass, epoxy resin and structural adhesive, cores and coating.

Prototype A – Hand Lay-Up Manufacturing Process

The manufacturing method for Prototype A involves using an expanded polystyrene (EPS) core covered with a biaxial fiberglass (BX-FG) layer impregnated with epoxy resin, as illustrated in Figure 4. This process results in the fabrication of a single-piece VAWT blade.

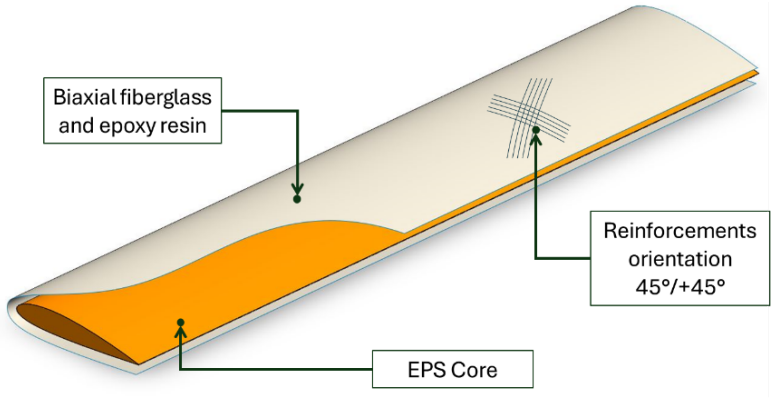

Figure 4. Structural design of Prototype A.

The hand lay-up manufacturing process for prototype A is described as follows:

A-1) Prototype A – Core Preparation (EPS Material)
A piece of EPS, corresponding to the full blade length (2 m), is shaped using wooden templates representing the NACA 0015 airfoil profile at each cross-section. Lateral wooden panels are also attached to form a bolted frame, as illustrated in Figure 5-(a). The EPS core is then cut using a hot wire guided by the wooden profiles on both the upper and lower sides, resulting in a finished EPS core with a total mass of 1.1 kg.

A-2) Prototype A – Laminate Application
The EPS core is covered with biaxial fiberglass (BX-FG) oriented longitudinally to ensure proper epoxy resin impregnation and uniform adhesion of the fibers across the entire surface of the core, as illustrated in Figure 5-(b).

(a) **(b)**

Figure 5. (a) Wood guides for EPS core, and (b) Biaxial fiberglass on EPS core.

The mass of the BX-FG before resin impregnation is 0.71 kg, calculated as the product of the layer's area density and total surface area, as shown in Equation 1. An additional 3 cm is added to the width of the BX-FG layer to ensure complete coverage of the EPS core. The biaxial fiberglass (BX-FG) has a standard surface density of 830 g/m², according to the manufacturer SAERTEX.

$$m_{BD-FG} = (0.83kg\ /\ m^2\ )(2\ m)(0.43\ m) = 0.71\ kg \quad \textbf{(1)}$$

In a manual lamination process, an additional percentage of epoxy resin must be considered, as this method provides less control over resin impregnation and the fiber volume fraction (FvF).

Prototype A – Epoxy resin impregnation and curing

A-3) The total epoxy resin matrix used for Prototype A is 1.2 kg, including an allowance for excess. After manual impregnation, the prototype is placed in a curing oven. This curing process, conducted at a constant temperature of 80 °C for 10 hours, ensures optimal mechanical properties of the composite. The curing parameters follow the recommendations of the resin manufacturer, KUKDO CHEMICAL HQ (KUKDO, 2011).

Prototype A – Surface finishing

A-4) Once the curing procedure is done, the surface imperfections must be examined, considering a repairing process on the surface of prototype A due to the sliding of the epoxy resin matrix by the effects of gravity. A rough surface is obtained by the fiberglass filaments, which affects the aerodynamic performance (Bai et al., 2014).

For the repairing process, a layer of epoxy filler is applied to the surface, which must cover the defects without modifying the aerodynamic surface. The total mass of the epoxy filler for prototype A is 1.45 kg.

A-5) To protect the composite from degradation by solar radiation a coating is necessary, the painting process uses a polyurethane paint. The total coating mass is 0.65 kg, which is applied with a paint spray gun. The list of materials for prototype A is shown in Table 3.

Table 3. List of materials for prototype *A*

Material	**Commercial data**
BX-FG	SAERTEX X-E-830 gsm (SAERTEX, 2022)
Epoxy resin matrix	KUKDO epoxy systems (KUKDO, 2011)
EPS core	FANOSA EPS
Epoxy filler	-
Coating	Polyurethane paint COMEX (COMEX, 2024)

Prototype B – VARTM Manufacturing Process

In Prototype B, the blade is composed of two separate parts: an upper shell (shell 1) and a lower shell (shell 2), which are bonded together using an epoxy structural adhesive. Unidirectional fiberglass (UD-FG) with an area density of 1180 g/m² and biaxial fiberglass (BX-FG) with an area density of 830 g/m², both supplied by SAERTEX, were used in the design of this prototype (see Figure 6).

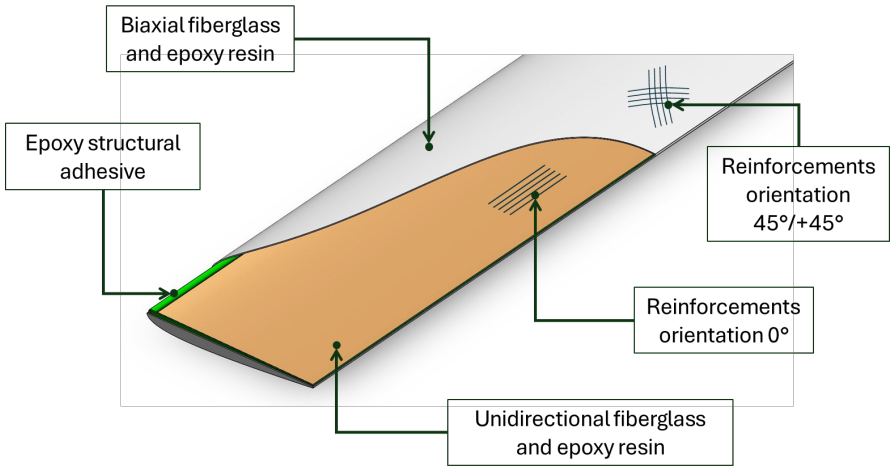

Figure 6. Structural design of prototype B.

Prototype B – Mold preparation

B-1) For the manufacture of Prototypes B, a master plug and mold were created. The master plug was fabricated from MDF sheets, which were bonded with glue to form an MDF block. This block was then machined using a CNC machine to produce the surface profile of the blade, see Figure 7-(a). The mold was subsequently created from the master plug, see Figure 7-(b).

(a) **(b)**

Figure 7. (a) Master plug machined with CNC machine, and (b) Mold for 1 kW VAWT blade.

B-2) The structural lamination for prototypes B consists of 4 layers of fiberglass per shell, with careful control of the filament orientation in each layer. Lamination begins with three layers of biaxial fiberglass (BX-FG), followed by a final layer of unidirectional fiberglass (UD-FG) placed directly on the mold surface, as illustrated in Figure 8.

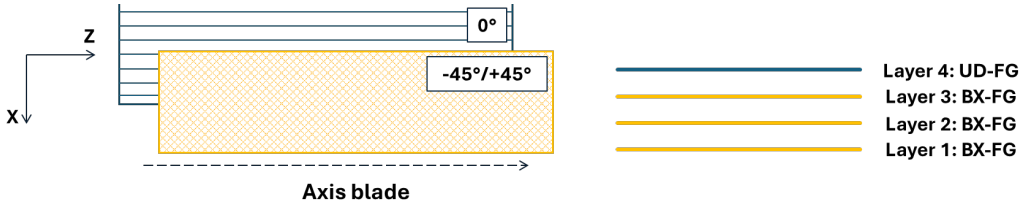

Figure 8. Reference alignment system for fiberglass layer lamination.

The total mass of the dry fiberglass layers is 1.55 kg for each shell. The mass of a single BX-FG layer is 0.35 kg, while the UD-FG layer has a mass of 0.5 kg.

Prototype B – VARTM process Set-up

B-3) After stacking the fiberglass layers, the consumables required for the VARTM process are positioned, as shown in Figure 9-(a). Based on a fiber volume fraction (FvF) of 100:50 for the infusion process, the total mass of the epoxy resin matrix is 0.78 kg per shell. During resin infusion, any vacuum-bag leaks should be checked and minimized before allowing the epoxy resin to enter the mold, see Figure 9-(b).

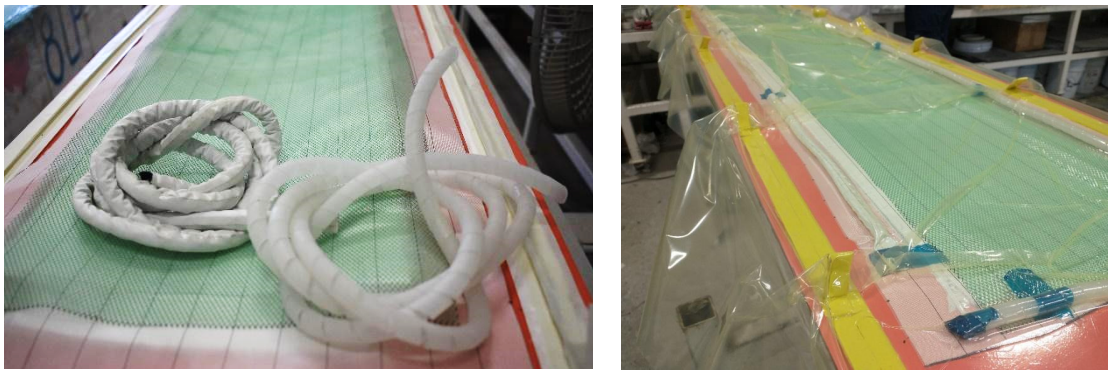

(a) **(b)**

Figure 9. (a) Consumables for the VARTM process, and (b) Vacuum-bag leakage inspection.

B-4) After the resin infusion is complete, each shell is placed in an oven for curing at 80 °C for 10 hours. Once the shells are fully cured, the consumables are removed in preparation for the trimming process, see Figure 10.

Figure 10. Inspection of the surface of the shell prototype B.

B-5) A bond line of epoxy structural adhesive, with a total mass of 0.5 kg, is applied along the inner perimeter of Shell 1. Shell 2 is then placed over Shell 1, carefully aligning the leading and trailing edges, and uniform pressure is applied across the entire surface to ensure proper bonding. Similar to the curing of the epoxy resin matrix, the epoxy structural adhesive undergoes a curing process in an oven at 80 °C for 10 hours.

B-6) During the bonding process, some epoxy structural adhesive bled around the blade. This excess material must be carefully removed without altering the blade geometry, particularly at the leading and trailing edges.

The total mass of the coating is 0.65 kg, the same amount as prototype A. The list of materials for prototype B is shown in Table 4.

Table 4. List of materials for prototype B.

Material	Commercial data
UD-FG	SAERTEX U-E-1180 gsm (SAERTEX, 2022)
BX-FG	SAERTEX X-E-830 gsm (SAERTEX, 2022)
Epoxy resin matrix	KUKDO epoxy systems (KUKDO, 2011)
Epoxy structural adhesive	HEXION EPIKOTE™ MGS™ BPR 135G-Series (HEXION/Westlake Epoxy, 2023)
Coating	Polyurethane paint COMEX (COMEX, 2024)

Prototype C – VARTM Manufacturing Process

Prototype C involves the integration of a shear-web element by replacing the EPS core of Prototype B with a polyurethane (PU) core. This modification results in an increase in weight due to the added structural adhesive and epoxy resin. Prototype C follows the same four-layer fiberglass lamination as Prototype B. This PU core functions as a shear-web, providing an additional bonding point and enhancing the stiffness of the blade, as illustrated in Figure 11. The PU core includes an internal fiberglass bridge that further increases the stiffness of the composite structure (SAERTEX, 2022).

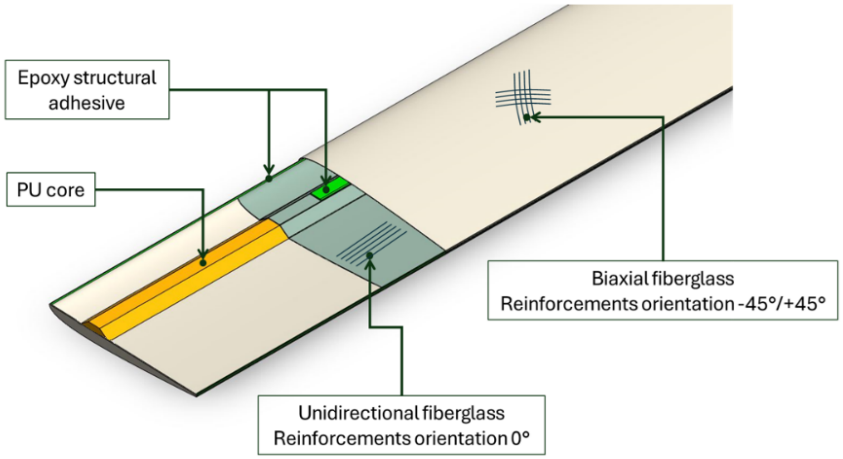

Figure 11. Structural design of prototype C

C-1) The manufacturing process of Prototype C is identical to that of Prototype B. After stacking and aligning the three BX-FG layers on the mold, the PU core is placed prior to adding the UD-FG layer, which is aligned with the pitch axis of the blade and centered on the PU core. The PU core has a geometry of 2 m in length, 75 mm in width, and 10 mm in thickness, as illustrated in Figure 12. The PU core is covered with a UD-FG layer, verifying that it does not move from its position. The PU core has a density of 214 kg/m^3, this material gives an extra mass to the entire shell of 0.32 kg.

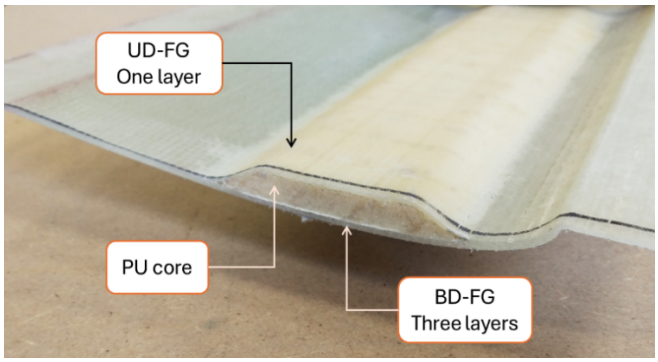

Figure 12. PU core lamination of prototype C.

The total mass of a BX-FG layer is 2.1 kg and for UD-FG it is 1.4 kg. The total mass of the dry fiberglass layers is 3.5 kg for the entire shell.

C-2) Based on a fiber volume fraction (FvF) of 100:50 for the infusion process, the total mass of the epoxy resin matrix for each shell is 1.75 kg. The VARTM process was performed following the same procedure as for Prototype B, using the same consumable arrangement for resin infusion and a curing process of 10 hours at 80 °C for each shell.

C-3) or Prototype C, bond lines of epoxy structural adhesive were applied to the inner surface of Shell 1. The first bond line was applied along the perimeter, and the second bond line was applied along the PU core section, as illustrated in Figure 13. The second bond line provides adhesion with Shell 2 and simulates the shear-web within the blade. The total mass of structural adhesive used is 1.0 kg. The curing process was carried out at 80 °C for 10 hours. Shell 2 is then placed over Shell 1, and uniform pressure is applied across the entire surface to ensure proper bonding. Any excess epoxy structural adhesive that bled around the edges is removed during the trimming process. A complete list of materials used for Prototype C is presented in Table 5.

The total mass of the coating of prototype C is 0.65 kg, the same amount as prototype A.

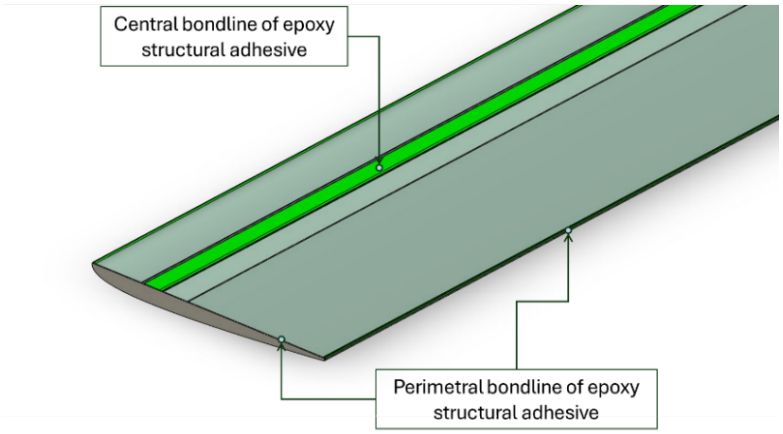

Figure 13. Epoxy structural adhesive bond lines.

Table 5. List of materials for prototype C.

Material	Commercial data
UD-FG	SAERTEX U-E-1180 gsm (SAERTEX, 2022)
BX-FG	SAERTEX X-E-830 gsm (SAERTEX, 2022)
Epoxy resin matrix	KUKDO epoxy systems (KUKDO, 2011)
PU core	SAERfoam ® 80 Series (SAERTEX, 2022)
Epoxy structural adhesive	HEXION EPIKOTE™ MGS™ BPR 135G-Series (HEXION/Westlake Epoxy, 2023)
Coating	Polyurethane paint COMEX (COMEX, 2024)

Results and Discussion

Mass results

Based on the data obtained from each manufactured prototype, the total mass of each prototype is presented in the Table 6.

Comparing the mass of individual materials and the total mass of each prototype, Prototype A is the lightest at 5.11 kg, Prototype B has a total mass of 5.81 kg, and Prototype C is the heaviest at 7.22 kg. The difference in mass between Prototype A, manufactured manually, and Prototype B, produced using the VARTM method, represents an increase of approximately 13%; while the inclusion of the internal reinforcement in Prototype C results in an increase of approximately 41%.

Table 6. Comparison of materials masses for prototypes A, B and C.

Material	Prototype A	Prototype B	Prototype C
UD-FG	-	1.00 kg	1.40 kg
BX-FG	0.71 kg	2.10 kg	2.10 kg
Epoxy resin matrix	1.20 kg	1.56 kg	1.75 kg
EPS core	1.10 kg	-	-
PU core	-	-	0.32 kg
Epoxy filler	1.45 kg	-	-
Epoxy structural adhesive	-	0.5 kg	1.00 kg
Coating	0.65 kg	0.65 kg	0.65 kg
Total	**5.11 kg**	**5.81 kg**	**7.22 kg**

Comparing Prototypes B and C, the increase in mass is attributed to the additional UD-FG layer, the increased epoxy resin required for the PU core, the PU core itself, and the second bond line. Prototype C has approximately 24% greater mass than Prototype B, considering that both prototypes were fabricated using the VARTM process and with a controlled fiber volume fraction (FvF) of 100:50.

Furthermore, the integration of the shear-web component in Prototype C results in a twofold increase in the mass of epoxy structural adhesive.

Cost analysis

The commercial materials used in the manufacture of these prototypes are considered specialized, as they are intended for wind industry applications and are certified by Det Norske Veritas (DNV) and Germanischer Lloyd (GL). Mexico does not have domestic manufacturers capable of supplying these materials; consequently, the associated costs are higher compared to other countries and relative to standard commercial fiberglass and resin matrices.

Based on the list of materials for each manufactured prototype, the corresponding cost percentages are presented in Table 7.

Table 7. Comparison of manufacturing cost percentages for Prototypes A, B, and C. Costs referenced to 2024

Material	Prototype A	Prototype B	Prototype C
UD-FG	0%	12%	17%
BX-FG	9%	27%	27%
Epoxy resin matrix	67%	87%	97%
EPS core	6%	0%	0%
PU core	0%	0%	7%
Epoxy filler	3%	0%	0%
Epoxy structural adhesive	0%	74%	148%
Coating	15%	15%	15%
Total	**100%**	**215%**	**312%**

When comparing the cost of each prototype, Prototype A is used as the cost reference. From this, it can be deduced that Prototype B costs more than twice as much as Prototype A, while Prototype C is nearly three times the cost. The

difference between Prototypes B and C is approximately one-third, which accounts for the inclusion of the PU core and the corresponding increases in structural adhesive and UD fiberglass.

According to Table 7, the epoxy resin used in Prototype A is the most expensive component. For Prototype B, the costs are distributed between the resin and the structural adhesive. In contrast, for Prototype C, the resin accounts for approximately one-third of the total cost, while the structural adhesive represents nearly half of the total cost. This could be one of the reasons why hundreds of thousands of euros are invested in Europe for research and technological development of structural adhesives for use in composite materials in the offshore energy and aerospace industries (Budzik et al., 2021). From the same table, it can be observed that the costs associated with the cores (EPS and PU) and the epoxy filler have a minimal impact on the total cost, while the coating is consistent across all prototypes. A notable difference lies in the number and type of fibers required to ensure structural strength, which is beyond the scope of this document.

Based on the hand lay-up and VARTM processes for blade manufacturing, several key characteristics of each process can be identified, as summarized in Table 8.

Table 8. Comparison of the VAWT blade prototype manufacturing process.

Parameter	**Hand lay-up process**	**VARTM process**
Mass	For the hand lay-up process (Prototype A), the fiber volume fraction (FvF) ratio used was 100:169, meaning that for every 100% of fiber mass, an additional 169% of resin mass was required. Therefore, any prototype manufactured by the manual method will primarily depend on the determination of its reinforcement mass (UD and BX fiberglass).	In the VARTM process, the FvF ratio is maintained at 100:50, and this relationship can be effectively controlled by the vacuum applied during the infusion setup. In other words, 100% of the fiber mass is complemented by only 50% of the resin mass.
Costs and materials	This method does not require specialized laboratories, equipment, or tools. It also allows the use of non-structural fibers (short fiber reinforcements) and different types of resins (e.g., polyester).	Structural fiberglass (continuous fiber reinforcements) and consumables significantly increase the manufacturing cost. In addition, the VARTM process requires a specialized facility equipped with tools and equipment such as vacuum pumps, a trimming room, a curing oven, and a storage room for materials.
Manufacturing time	The manufacturing time is relatively short. For Prototype A, the total manufacturing time was 32 hours, including the surface repair with epoxy filler and the painting process.	For the VARTM process, the manufacturing time of each prototype (B and C) was 48 hours, as this method involves more steps in blade fabrication. Prototype C required an additional 2 hours due to the integration of the PU core.
Surface quality	For Prototype A, surface repair was necessary because the epoxy resin slid due to the effects of gravity before curing, as shown in Figure 14-(a). This repair increased the mass to 1.45 kg, generating an imbalance.	The VARTM process delivers a shell with fewer defects, requiring only minor repairs, as shown in Figure 14-(b). In addition, the vacuum bag ensures uniform impregnation of the epoxy resin matrix into the glass fiber layers.

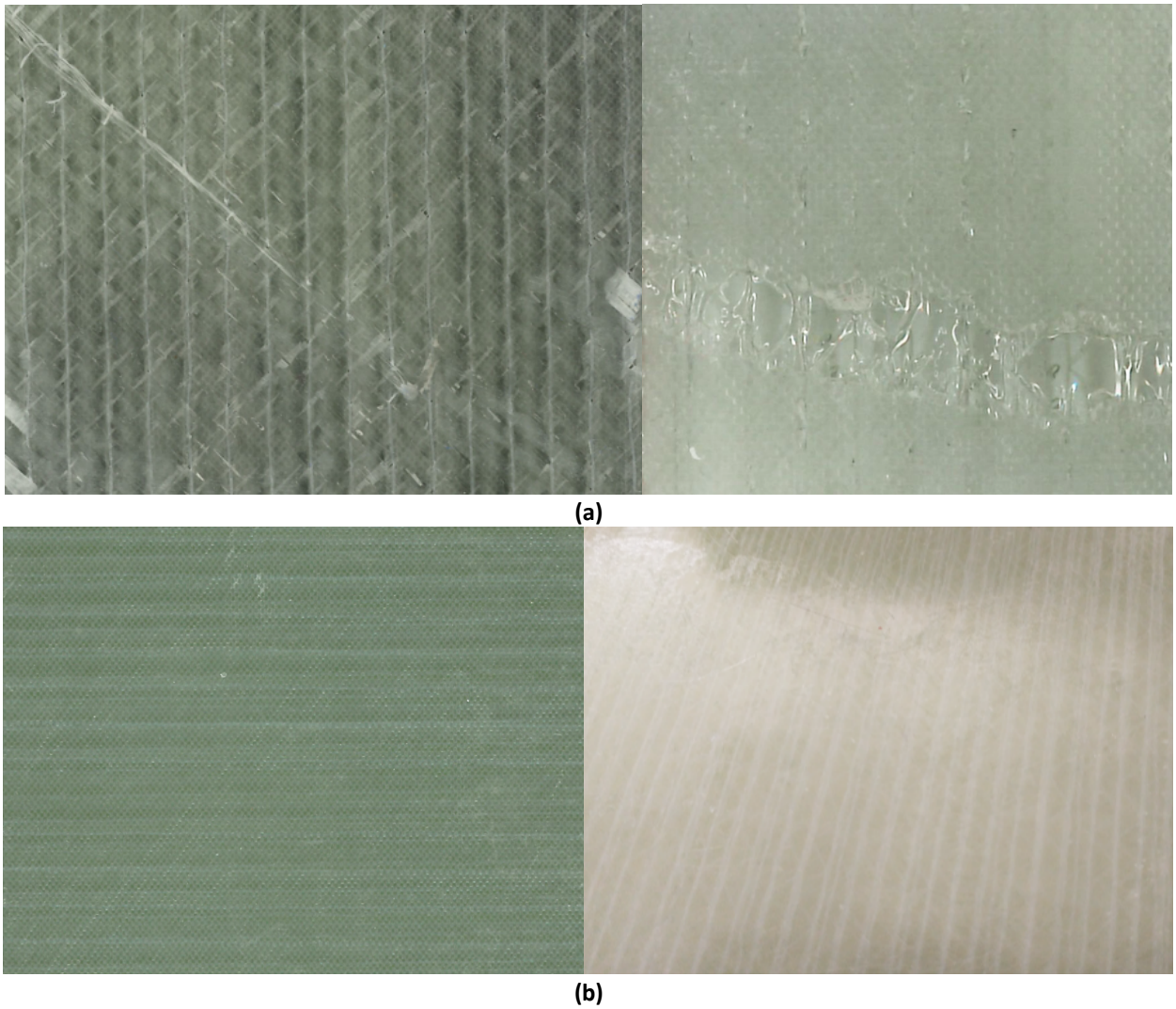

Figure 14. (a) Hand lay-up external surface quality, and (b) VARTM external surface quality.

Conclusions

This research compared the mass, cost, and surface quality of three VAWT blade prototypes, manufactured using both hand lay-up and Vacuum Assisted Resin Transfer Molding (VARTM) processes, with the goal of identifying the material costs and mass of the blades in order to optimize their manufacturing process.

Key findings regarding mass indicated that Prototype A, produced via hand lay-up with an EPS core, was the lightest at 5.11 kg. Prototypes B and C, both manufactured using the VARTM process, were successively heavier. Prototype B, without a shear web, weighed 5.81 kg, an approximate 13% increase over Prototype A. Prototype C, which incorporated a polyurethane (PU) core as a shear web, was the heaviest at 7.22 kg, representing an increase of about 41% compared to Prototype A and 24% compared to Prototype B. The added mass in Prototype C was attributed to the additional unidirectional fiberglass (UD-FG) layer, increased epoxy resin for the PU core, the PU core itself, and a twofold increase in epoxy structural adhesive mass for the second bond line.

In terms of cost, the hand lay-up process (Prototype A) was the most economical, serving as the cost reference (100%). The VARTM process significantly increased manufacturing expenses, with Prototype B costing 215% and Prototype C nearly three times as much (312%) as Prototype A. Specialized commercial materials, not domestically manufactured in Mexico, contributed to these higher costs. For Prototype A, the epoxy resin was the most expensive component. In contrast, for VARTM prototypes, the costs were distributed between the epoxy resin matrix and, notably, the epoxy structural adhesive, which accounted for almost half of Prototype C's total cost due to the shear web integration. Cores

(EPS and PU) and epoxy filler had a minimal impact on the total cost, while coating costs were consistent across all prototypes.

Regarding manufacturing process characteristics and quality, the hand lay-up method (Prototype A) required less specialized equipment and was generally faster (32 hours) but resulted in a rough surface due to gravity-induced resin sliding, necessitating surface repair with epoxy filler and leading to a high resin-to-fiber ratio (FvF of 100:169). Conversely, the VARTM process (Prototypes B and C) yielded shells with superior surface quality and fewer defects, largely due to uniform resin impregnation ensured by the vacuum bag and controlled FvF (100:50). However, VARTM required specialized facilities, more consumables, and a longer manufacturing time (48 hours for B and 50 hours for C), contributing to its higher cost.

This study underscores a critical trade-off between manufacturing cost and blade mass. While hand lay-up offers a cost-effective solution for lighter blades, it compromises on surface quality and precise material control. VARTM, though more expensive and resulting in heavier blades (especially with structural enhancements), delivers superior quality and better material utilization, which are vital for enhancing efficiency and durability. The significant cost contribution of structural adhesives highlights an area for future research and development to potentially reduce overall manufacturing expenses in high-performance composite applications, echoing investment trends observed in Europe. Ultimately, the choice of manufacturing process should align with the specific performance requirements and economic constraints of VAWT applications, particularly those intended for challenging urban environments or offshore installations.

Considering that the criteria for selecting the optimal option are manufacturing quality, low cost, and minimal mass, based on the findings of Vidal-Flores and Hernández-Arriaga (2024), which show that lower blade mass enables rotor start-up at lower wind speeds, Prototype B was selected as the best option for the fabrication of an H-type VAWT rotor, with an average mass of 5.81 kg per blade. It is important to mention that the mechanical characterization of the proposed blades through static and dynamic tests is part of another practical study aimed at confirming theoretical concepts. The VARTM process allows for standardized and more controlled surface quality improvements compared to the hand lay-up method, which relies on manual lamination and must be adapted for each individual piece. Furthermore, the cost of Prototype B could potentially be reduced by approximately 30% through a redesigned manufacturing process, which is currently under investigation and includes a patent proposal for ultralight, one-shot blades to be reported in future work.

Other options to enable the development of VAWT blade designs with different materials, such as natural fibers (sisal, flax, hemp, jute, etc) are under research focusing on reuse after their life cycle. The goal remains to reduce costs and implement advanced technologies in composite manufacturing processes, while also introducing a circular economy for VAWTs. This approach aims to make these turbines more accessible and affordable for use in urban environments.

Acknowledgments and Funding: The authors would like to thank the Laboratorio de Innovación en Energía Eólica de CIATEQ A. C. Bernardo Quintana Querétaro unit for allowing the use of its facilities and equipment for the development of this work and the Secretaría de Ciencia, Humanidades, Tecnología e Inoovación (SECIHTI).

Author contributions: G.V.-F.: writing, conceptualization, provide materials, design, editing, supervision, project administration; F.Q.-E.: writing, analysis and interpretation of data, conceptualization, provide materials, design, data collection, editing. J.R. G-B: manufacture of prototypes, provide materials, analysis and interpretation of data, writing, editing. I.A.-M: manufacture of prototypes, provide materials, analysis and interpretation of data, writing, editing.

References

Alvarado, M. I. (2023). Análisis aeroelástico de detalle para el rediseño estructural del laminado con materiales compuestos de un aspa para un aerogenerador de 30 kW. UAEMéx: Universidad Autónoma del Estado de México.

Bai, T., Liu, J., Zhang, W., & Zou, Z. (2014). Effect of surface roughness on the aerodynamic performance of turbine blade cascade. *Propulsion and Power Research*, *3*(2), 82–89, https://doi.org/10.1016/j.jppr.2014.05.001

Boo, S.Y., Shelley, S.A., Griffith, D.T., & Escalera Mendoza, A.S. (2023). Responses of a Modular Floating Wind TLP of MarsVAWT Supporting a 10 MW Vertical Axis Wind Turbine. *Wind*, 3, 513–544, https://doi.org/10.3390/wind3040029

Brandetti, L. (2024). Design for urban vertical-axis wind turbines: balancing performance and noise. TU Delf: Delft University of Technology, https://doi.org/10.4233/uuid:812de44e-36fb-4e5d-acf7-973f38d965de

Budzik, M. K., Wolfahrt, M., Reis, P., Kozłowski, M., Sena-Cruz, J., Papadakis, L., Nasr Saleh, M., Machalicka, K. V., Teixeira de Freitas, S., & Vassilopoulos, A. P. (2021). Testing mechanical performance of adhesively bonded composite joints in engineering applications: an overview. *Journal of Adhesion*, *98*(14), 2133-2209, https://doi.org/10.1080/00218464.2021.1953479

Chawla, K. K. (2019). Composite materials: science and applications (4th ed). Springer.

COMEX. (2024). Carta técnica: U-10 Recubrimiento de Poliuretano de Altos Sólidos. [Archivo PDF], https://www.comex.com.mx/getattachment/f5bca495-8d9a-42d2-92e8 a83c9ce7292c/.aspx/. Consultado el 24 de febrero de 2024.

Cuevas-Carvajal, N., et al. (2022). Effect of geometrical parameters on the performance of conventional Savonius VAWT: A review. *Renewable and Sustainable Energy Reviews*, 161, 112314, https://doi.org/10.1016/j.rser.2022.112314

Devin, M., Mendoza, N., Platt, A., Moore, K., Jonkman, J., & Ennis, B. (2023). Enabling Floating Offshore VAWT Design by Coupling OWENS and OpenFAST: Article No. 2462. *Energies*, *16*(5), https://doi.org/10.3390/en16052462

Edwards, E. C., Holcombe, A., Brown, S., Ransley, E., Hann, M., & Greaves, D. (2024). Trends in floating offshore wind platforms: A review of early-stage devices. *Renewable and Sustainable Energy Reviews*, *193*, 114271, https://doi.org/10.1016/j.rser.2023.114271

Geneid, A.A., Atia, M.R.A. & Badawy, A. (2022). Multi-objective optimization of vertical-axis wind turbine's blade structure using genetic algorithm. *Journal of Engineering and Applied Science, 69*, 90, https://doi.org/10.1186/s44147-022-00150-z

Ghigo, A., Faraggiana, E., Giorgi, G., Mattiazzo, G., & Bracco, G. (2024). Floating Vertical Axis Wind Turbines for offshore applications among potentialities and challenges: A review. *Renewable and Sustainable Energy Reviews*, 193, 114302, https://doi.org/10.1016/j.rser.2024.114302

Gurit. (2016). Guide to Composites: Delivering the future of composite solutions. Gurit

HEXION/Westlake Epoxy. (2023). Technical data sheet: EPIKOTETM Resin MGS ® 135G-Series

IEC. (2013). IEC 61400-2 Wind turbines – Part 2: Small wind turbines (edition 3.0).

IRENA. (2012). RENEWABLE ENERGY TECHNOLOGIES: COST ANALYSIS SERIES – Volume 1: Power sector Issue 5/5 Wind Power, https://www.irena.org/-/media/Files/IRENA/Agency/Publication/2012/RE_Technologies_Cost_Analysis-WIND_POWER.pdf. Consultado el 24 de octubre de 2024.

Juan, Y., Rezaeiha, A., Montazeri, H., Blocken, B., & Yang, A. (2024). Improvement of wind energy potential through building corner modifications in compact urban areas. *Journal of Wind Engineering and Industrial Aerodynamics*, *248*, 105710, https://doi.org/10.1016/j.jweia.2024.105710

KUKDO. (2011). Technical data sheet: KUKDO Epoxy systems for composites. KUKDO CHEMICAL. CO., LTD.

Lee, C.H., Khalina, A., Nurazzi, et al (2021). The Challenges and Future Perspective of Woven Kenaf Reinforcement in Thermoset Polymer Composites in Malaysia: A Review. *Polymers*, *13*, 1390, https://doi.org/10.3390/polym13091390

Marinić-Kragić, I., Vučina, D., & Milas, Z. (2022). Robust optimization of Savonius-type wind turbine deflector blades considering wind direction sensitivity and production material decrease. *Renewable Energy*, *192*, 150-163, https://doi.org/10.1016/j.renene.2022.04.118

Marzec, Ł., Buliński, Z., Krysiński, T., & Tumidajski, J. (2023). Structural optimisation of H-Rotor wind turbine blade based on one-way Fluid Structure Interaction approach. *Renewable Energy*, *216*, 118957, https://doi.org/10.1016/j.renene.2023.118957

Mendoza, V., Katsidoniotaki, E., & Bernhoff, H. (2020). Numerical Study of a Novel Concept for Manufacturing Savonius Turbines with Twisted Blades *Energies, 13*(8), 1874, https://doi.org/10.3390/en13081874

SAERTEX. (2022). Structural core material. [Archivo PDF], https://www.saertex.com/en/support/downloads. Consultado el 10 de febrero de 2022.

SAERTEX. (2022). Technical data sheet: U-E-1182g/m2-1270mm. [Archivo PDF], https://www.saertex.com/en/products/datasheet-glass. Consultado el 10 de febrero de 2024.

SAERTEX. (2022). Technical data sheet: X-E-832g/m2-1270mm. [Archivo PDF], https://www.saertex.com/en/products/datasheet-glass. Consultado el 10 de febrero de 2024.

Stoevesandt, Bernhard & Schepers, Gerard & Fuglsang, Peter & Yuping, Sun. (2020). Handbook of Wind Energy Aerodynamics. Springer.

Vidal-Flores, G., & Hernandez-Arriaga, I. (2024). Optimización aerodinámica para mejorar el par de arranque de una Turbina de Viento de Eje Vertical Savonius-Darrieus de 1 kW. *Revista Ingeniería Mecánica Tecnología y Desarrollo, 7*(5), 109-119. https://doi.org/10.59920/rimtd.20241m